

ChemComm

Accepted Manuscript



This is an *Accepted Manuscript*, which has been through the Royal Society of Chemistry peer review process and has been accepted for publication.

Accepted Manuscripts are published online shortly after acceptance, before technical editing, formatting and proof reading. Using this free service, authors can make their results available to the community, in citable form, before we publish the edited article. We will replace this *Accepted Manuscript* with the edited and formatted *Advance Article* as soon as it is available.

You can find more information about *Accepted Manuscripts* in the [Information for Authors](#).

Please note that technical editing may introduce minor changes to the text and/or graphics, which may alter content. The journal's standard [Terms & Conditions](#) and the [Ethical guidelines](#) still apply. In no event shall the Royal Society of Chemistry be held responsible for any errors or omissions in this *Accepted Manuscript* or any consequences arising from the use of any information it contains.



Direct Production of Naphthenes and Paraffins from Lignin

Jiechen Kong,^a Mingyuan He,^a Johannes A. Lercher^{*b} and Chen Zhao^{*a}

Received 00th xx 20xx,
Accepted 00th xx 20xx

DOI: 10.1039/x0xx00000x

www.rsc.org/

Utilization of lignin as a fuel precursor attracts attention, and a novel and facile process is developed for one-pot conversion of lignin to cycloalkanes and alkanes with Ni catalysts at moderate condition. This cascade hydrodeoxygenation approach may open a new promising technique for direct liquefaction of lignin to hydrocarbons.

Selective and efficient conversion of lignocellulose to fuels and chemicals is considered to be the greatest challenge in modern catalysis.¹⁻⁴ Lignin, the second abundant lignocellulose resource, is rich in aromatic rings and energy density that make it attractive as a promising renewable bio-resource to generate fuels and chemicals.⁵ However, the complexity of its three-dimensional cross-linking polymeric structure leads to its low solubility in conventional organic solvents, as well as small collision possibility of C-O-C linkage with active catalytic sites. These specific properties of lignin make it difficult to be converted.⁶

The C-O cleavage of lignin derived model compounds, such as phenolic monomers⁷⁻¹⁰ and dimers¹¹⁻¹⁶, are widely investigated by sulfided and reduced metal catalysts. However, these catalytic systems working well with model compounds are tested to be not propitious or proper for real polymeric lignin deconstruction. The efforts for lignin depolymerization, especially for breaking down the much weaker C-O bonds in lignin, are mainly aimed at routes of hydrolysis¹⁷, ethanolysis¹⁸, oxidation¹⁹, and reduction²⁰⁻²⁴. It is notable that recently Stahl and co-workers develop a two-stage process for depolymerization of an oxidized lignin in aqueous formic acid to give a high yield of monomeric phenolics (61 wt%) under mild conditions¹⁷. However, the current techniques for depolymerization of crude lignin are still far from the requirement

of high efficiency and high selectivity. In principle, it would be a better strategy that hydrocarbons can be directly produced from lignin.

In this work, we establish a new process for one-pot converting of lignin to hydrocarbons (with nearly 50% yield and 100% selectivity) using a non-precious Ni catalyst supported on amorphous silica alumina at moderate conditions. The developed Ni based catalysts exert multi-function, including cleaving of the exposed external C-O-C linkages of lignin, sequentially breaking down the C_{aromatic}-O and C_{aliphatic}-O bonds in the produced phenolic oligomers, secondary and primary phenolic compounds, as well as removing of oxygen in Ph-OCH₃ and Ph-OH groups.

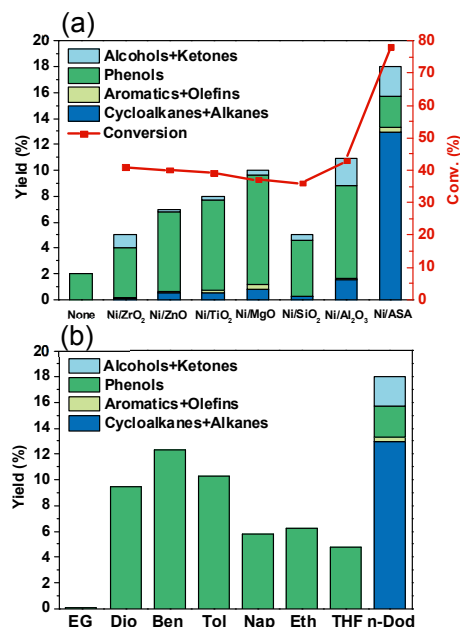


Figure 1. a). Conversion of lignin with supported Ni catalysts. b). Conversion of lignin in different solvents. EG: ethylene glycol, Dio: dioxane, Ben: benzene, Tol: toluene, Nap: naphthalene, Eth: ethanol, THF: tetrahydrofuran, n-Dod: dodecane. Reaction conditions: lignin (2.0 g), Ni/ASA catalyst (30.1 wt.%, 1.0 g), solvent (80 mL), 250 °C, 4 MPa H₂, 160 min., stirring at 700 rpm.

^a School of Chemistry and Molecular Engineering, East China Normal University, Shanghai 200062, China
E-mail: czhao@chem.ecnu.edu.cn

^b Department of Chemistry and Catalysis Research Center, TU München, Lichtenbergstraße 4, 85748 Garching, Germany
Institute for Integrated Catalysis, Pacific Northwest National Laboratory, 902 Battelle Boulevard, Richland, WA 99352, USA
E-mail: johannes.lercher@ch.tum.de

† Electronic Supplementary Information (ESI) available: [details of any supplementary information available should be included here]. See DOI: 10.1039/x0xx00000x

The used cellulolytic enzyme lignin originates from corncob after enzymatically hydrolyzing of cellulose and hemicellulose, attaining a Klason lignin content of 80 wt.% (Tables S1a and S1b). The soluble molecular weight of lignin attained an M_w/M_n value of 3061 ($M_n = 1.04$), as determined from the measurement of gel permeation chromatography (GPC). The elementary analysis suggested that the structure unit of lignin was $C_{10}H_{10.3}O_{3.8}$ with a molecular weight of $191 \text{ g}\cdot\text{mol}^{-1}$, and accordingly, lignin contained at least 19 structural units. Measurements of infrared and ^1H NMR spectroscopy manifested that lignin was rich in phenyl, guaiacyl, and syringyl unit structures (Fig. S1). The metallic Ni center showed high activities in conversion of phenolic monomers and dimers in water, but these developed catalyst systems were tested to be not suitable for real lignin conversion due to severe coke or tar formation.^{9,11} In the blank test at 250 °C in presence of 4.0 MPa hydrogen, only 2 wt.% liquid fragments were formed with 100% substituted phenols in dodecane after 160 min.. In addition, serious

coke was observed. Catalyzed by the 30 wt.% Ni/oxides catalysts (prepared by deposition precipitation method) at identical conditions, more than 90 kinds of products were detected, mainly including oxygenates, cycloalkanes, and aromatics (Table S2). The Ni catalysts, that is, supported on oxides of SiO_2 , Al_2O_3 , or ZrO_2 , ZnO , TiO_2 , and MgO , yielded a maximum liquid of 11 wt.%, leading to high concentrations of oxygenates formation. For example, Ni/ Al_2O_3 reached 84% selectivity of oxygenates (Fig. 1a).

In comparison, Ni supported on amorphous-silica-alumina (Ni/ASA) led to the highest lignin conversion at 78 wt.% with an 18 wt.% liquid yield (Fig. 1a), attaining a lignin conversion rate of $0.58 \text{ g}_{\text{lig}}\cdot\text{g}_{\text{cat}}^{-1}\cdot\text{h}^{-1}$ and a turnover frequency (TOF) of $17.4 \text{ mol}_{\text{lig}}\cdot\text{mol}_{\text{surf}}^{-1}\cdot\text{Ni}^{-1}\cdot\text{h}^{-1}$ (Ni dispersion: 3.5%, M_w lignin unit = $191 \text{ g}\cdot\text{mol}^{-1}$). The much lower liquid yield (18%) compared to the lignin conversion value (78%) maybe attributed to the undetected high molecular-weight phenolic oligomers by GC-GC×MS, whereas these heavier compounds were identified by HPLC-MS measurement (Fig. S3). It should be addressed that majorities of liquid products over Ni/ASA were alkanes and aromatic hydrocarbons (74% selectivity, Fig. 1a), with a small fraction of 26% oxygenates formation (phenols, ketones, and alcohol, Table S3). This indicated that the acidity especially the specific Brönsted acid sites on Ni/ASA ($0.107 \text{ mmol}\cdot\text{g}^{-1}$, Table S2) facilitate the oxygen removal from phenolic compounds and downstream oxygenate fragments, leading to the final hydrocarbons production. The relatively lower liquid yield (18 wt.%) compared to the high lignin conversion (78 wt.%) implied that transformation of the phenolic oligomers intermediate is the slowest step in the selected system.

The impact of solvents (Fig. 1b) revealed that Ni/ASA performed much better in apolar solvents (benzene, toluene, naphthane, and tetrahydrofuran) than in some polar solvents (ethylene glycol, ethanol, and dioxane). In fact dioxane and ethanol can well dissolve lignin, but Ni nano-clusters exert poorly due to their oxidation or instability in these polar solvents.²⁵ The highest liquid yield (18.0 wt.%) was achieved in dodecane (Fig. 1b). In addition, variation of temperatures from 250 °C to 320 °C in dodecane led to a liquid yield increase from 18.0 wt.% (conv: 52.9 wt.%) to 43.9 wt.% (conv: 79.0 wt.%) over Ni/ASA (Fig. 2a), proportional to a cycloalkane mixture yield from 13.0% to 42.0%. In parallel, an increase in H_2 pressure from 3.0 to 6.0 MPa enhanced the liquid yield from 30.1 wt.% (conv: 73.5 wt.%) to 46.2 wt.% (conv: 78.0 wt.%) at 300 °C (Fig. 2b). The liquid yields remarkably increase accompanied with nearly stable lignin conversions, suggesting that the enhanced temperatures and hydrogen pressures were beneficial for cleaving of lignin-derived phenolic oligomers to much smaller fragments.

The high activity of Ni nanoclusters was probably attributed to the high surface area of ASA ($S_{\text{BET}}: 292 \text{ m}^2\cdot\text{g}^{-1}$, Fig. 3a and Table S2) supported Ni nanoclusters with good dispersed (Fig. 3b) and with small sizes ($d = 6.5 \pm 2.1 \text{ nm}$ as determined by TEM image, see Fig. 3c) at a high loading (Ni content: 30 wt.%). The SEM image (Fig. 3d) also manifested a mesoporous external surface of Ni/ASA. Meanwhile, rates for lignin conversion were shown to be sensitive to Ni particle sizes (Fig. S4), as evidenced by the fact that the larger Ni particles (18 nm, calcined at 750 °C) reduced 50% liquid yield than smaller Ni particles (11 nm, calcined at 450 °C). The sensitivity of Ni size to lignin conversion efficiency was attributed to the fact that the in the initial stage small Ni nanoclusters attack external

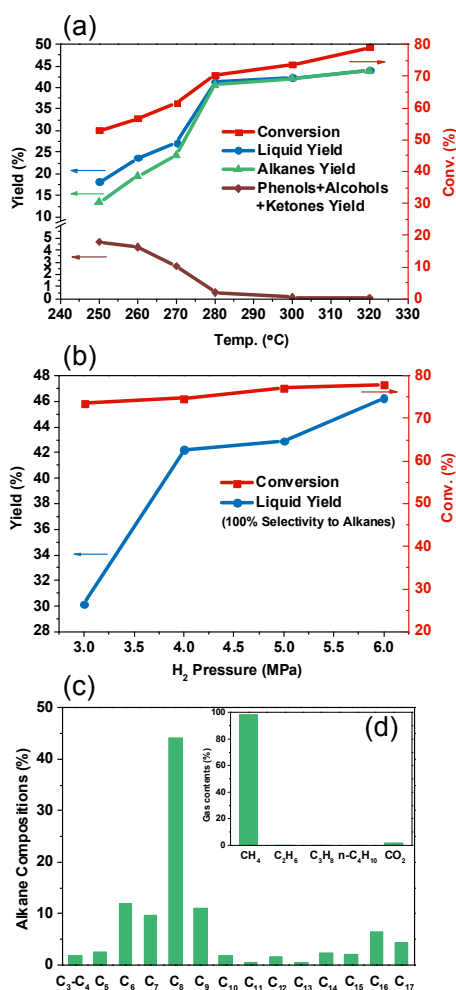


Figure 2. a) Temperatures and b) hydrogen pressures impact towards lignin conversion and product distributions. c) Alkane compositions in liquid phase and d) gas phase product distributions from lignin conversion at 300 °C in presence of 6 MPa H_2 . Reaction conditions: lignin (2.0 g), Ni/ASA catalyst (30.1 wt.%, 1.0 g), dodecane (80 mL), 160 min., stirring at 700 rpm.

exposed C-O-C linkages of lignin in dodecane as the first step. The Ni leaching was undetectable ($< \text{ICP detection limitation: 1 ppm}$) during the whole conversion.

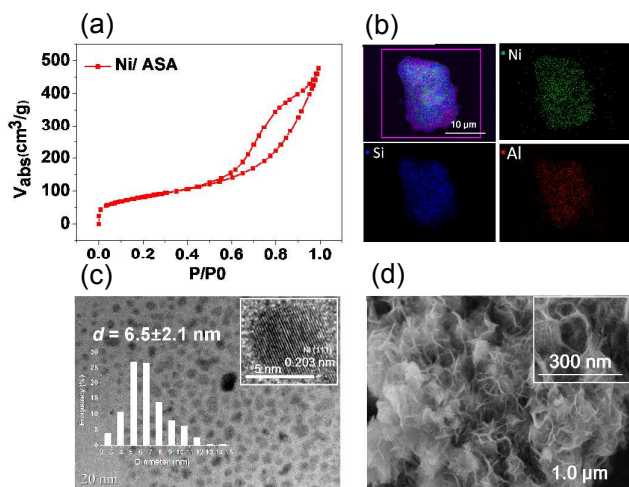


Figure 3. Characterization of Ni/ASA catalyst by a) N_2 adsorption and desorption isotherms, b) SEM-mapping image, c) TEM and d) SEM images.

Under optimized conditions ($300\text{ }^\circ\text{C}$ and 6.0 MPa H_2), the formed transparent liquid products (yield: 46.2%, Fig. 2c and Fig. S5) included a selectivity of 80.8% $\text{C}_3\text{-C}_9$ (gasoline range), as well as 6.5% $\text{C}_{10}\text{-C}_{14}$ (kerosene range) and 12.7% $\text{C}_{14}\text{-C}_{17}$ (diesel range) naphtha and paraffins (Fig. 4 and Table S4) affording nearly 100% selectivity of hydrocarbons, while small amounts of $\text{C}_3\text{-C}_6$ light alkanes as well as trace tetrahydropyran and 2-methyl tetrahydropyran were partly originated from residual cellulose and hemicellulose conversion (Table S4 and Fig. S6). Gaseous products consisted of 98% CH_4 and 2% $\text{C}_2\text{-C}_4$ light alkanes (Fig. 2d, Fig. S7).

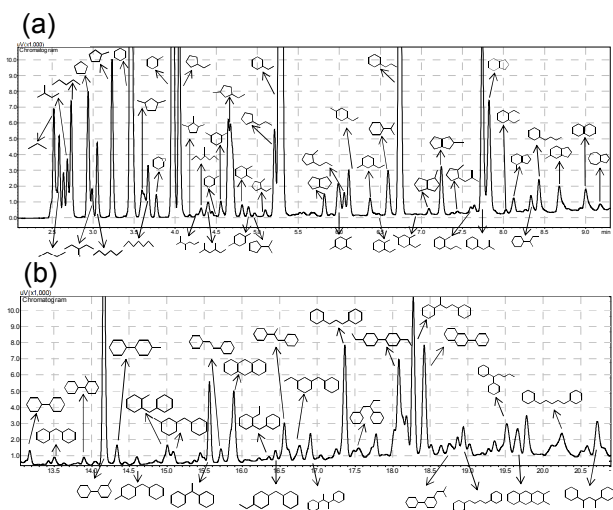


Figure 4. Liquid products of a) $\text{C}_3\text{-C}_{10}$ and b) $\text{C}_{12}\text{-C}_{17}$ hydrocarbons from one-pot lignin conversion over Ni/ASA. Conditions: lignin (2.0 g), Ni/ASA catalyst (30.1 wt.%, 1.0 g), dodecane (80 mL), $300\text{ }^\circ\text{C}$, 6 MPa H_2 , 160 min., stirring at 700 rpm.

The stability of Ni/ASA on converting of lignin was tested in four consecutive recycling runs (Fig. 5). After each reaction, the used catalyst was washed by dimethyl sulfoxide (DMSO) to dissolve the unreacted lignin feedstock, and was then sequential calcined in air, and reduced in hydrogen. After four runs, the lignin conversion, the liquid yield and the alkane selectivity still reached 74.3%, 40.1% and 92.1% respectively, quite approaching the activity obtained with the fresh catalyst. These data indicated that Ni/ASA catalyst possessed high durability in the selected catalytic system. The spent Ni/ASA catalyst was sequentially characterized by measurements of XRD, SEM, TEM, and N_2 adsorption (see supporting information Fig. S8). The slightly enlarged Ni nanoparticles ($d_{\text{TEM}} = 7.6 \pm 2.3\text{ nm}$) and the shrunk specific surface areas ($S_{\text{BET}} = 254\text{ m}^2\text{g}^{-1}$) of the used Ni/ASA catalyst may attribute to the small decrease of the hydrodeoxygenation activity during catalytic runs.

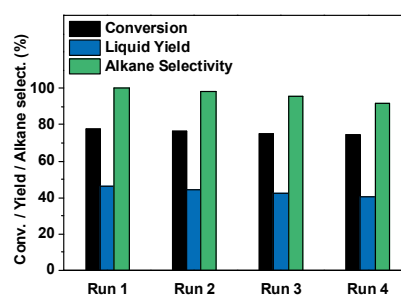


Figure 5. Recycling tests of lignin conversion over Ni/ASA. Conditions: lignin (2.0 g), Ni/ASA (30.1 wt.%, 1.0 g), dodecane (80 mL), $300\text{ }^\circ\text{C}$, 6 MPa H_2 , 160 min., stirring at 700 rpm.

To understand the individual steps in lignin depolymerization, the kinetics curve revealed that the cycloalkanes yields were increased up to 43% (with exceeding 80% selectivity) along with the reaction time (Fig. 6a), while the important intermediates of substituted phenols and cyclohexanols were increased to the maximum yields of respective 1.0% and 2.5% at 40 min., and subsequently decreased to zero as a function of time. These results indicated that the crucial fragments from lignin degradation were substituted phenols and alcohols, which were swiftly converted to final cycloalkanes and alkanes over Ni/ASA via complex cascade steps (Fig. 6b). To clarify the complex C-O bond cleavage process, the separate kinetics test of typical phenolic dimer linkage ($\beta\text{-O-4}$ model compounds) conversion was performed over Ni/ASA at identical conditions (Fig. S10a). It revealed that hydrogenolysis of $\text{C}_{\text{aliphatic-O}}$ and $\text{C}_{\text{aromatic-O}}$ bonds appeared as the primary step, and the sequential hydrodeoxygenation steps on phenol, 2-phenylethanol and aromatics fragments followed (Fig. S10a). The C-C coupling reaction (yield: 7.2%) was observed among phenolic intermediates via the alkylation route as well. Furthermore, the kinetics curves on guaiacol conversion over Ni/ASA (Fig. S10b) demonstrated that the parallel steps of removing of methoxy/hydroxy groups as well as hydrogenation of benzene-ring appeared as the initial step. The sequential dehydration, hydrogenolysis, and hydrogenation integrated steps on the formed cycloketone, cycloalcohols, and cyclic ether generated the final

cycloalkanes and alkanes (Fig. S10b). A variety of lignin-derived phenolic monomers and dimers were quantitatively converted to cyclic alkanes over Ni/ASA at selected conditions, as well (Fig. S11).

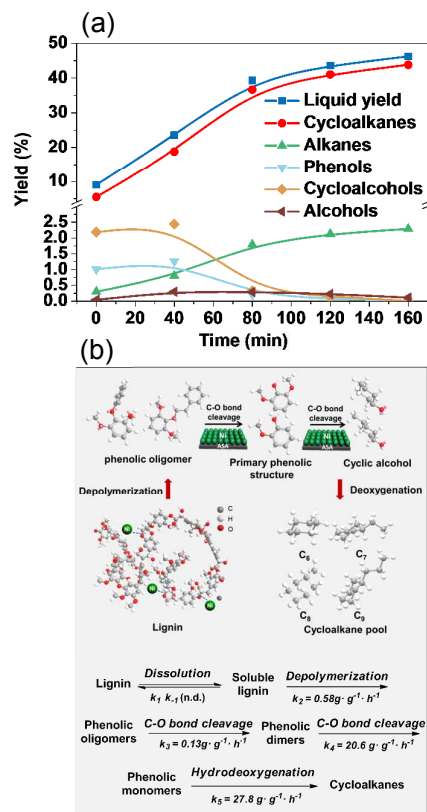


Figure 6. a) Kinetics of lignin conversion with Ni/ASA in the apolar solvent. Conditions: lignin (2.0 g), Ni/ASA catalyst (30.1 wt.%, 1.0 g), dodecane (80 mL), 300 °C, 6 MPa H_2 , stirring at 700 rpm. b) Reaction pathways in one-pot direct conversion of lignin to a mixture of cycloalkanes.

Combining these results allowed us to depict the overall reaction pathway for one-step conversion of cellulosytic enzyme lignin to cycloalkanes (Fig. 6b). Under appropriate conditions, lignin was dissolved in apolar solvent dodecane in equilibrium (k_1 , not determined), which fast shifts as lignin was consumed gradually. Subsequently, the small and uniform Ni nanoclusters supported on ASA cleaved the exposed external C-O-C linkages of the lignin macromolecule to form phenolic oligomers (k_2 , designated as the rate of lignin conversion). The multi-steps of C-O cleavage on phenolic oligomers follow (k_3 , designated as the rate of liquid yield formation from lignin). The sequential hydrogenolysis of phenolic dimers and trimers produces guaiacol and syringol derivatives (k_4). Followed by multi-steps of demethoxygenation, hydrogenation, and dehydration, guaiacol and syringol derivatives were converted to target cycloalkanes (k_5). Meanwhile, the hydrogenolysis of Ph-OCH₃ group produced the dominant CH₄ in the gas phase. Based on the kinetics of lignin (k_2 , k_3) as well as of typical phenolic monomer (k_5) and dimer conversion (k_4), it could be roughly estimated that the individual reaction rates follow the order (unit: $\text{g} \cdot \text{g}^{-1} \cdot \text{h}^{-1}$): k_5 (27.8) > k_4 (20.6) \gg k_2 (0.58) > k_3 (0.13), suggesting that the rate-determining step was the cleavage of phenolic oligomers.

In summary, we have developed a new and simple route for directly producing C₃-C₁₇ hydrocarbons from cellulosytic enzyme lignin with the non-precious metal Ni/ASA catalyst in apolar solvent via cascade steps in a one-pot process. These obtained naphthene and paraffin hydrocarbons are promising precursors to be further manufactured to clean fuels of gasoline, kerosene, diesel, as well as aromatics chemicals. We believe that the developed highly integrated new and efficient lignin transformation system can provide intrinsic insights for direct liquefaction of the abundant cellulosytic enzyme lignin, as well as inspiring thoughts in exploiting waste lignocellulose and sulfated/alkali lignin to produce value-added fuels and chemicals.

We gratefully acknowledge the financial support by the Recruitment Program of Global Young Experts in China, National Natural Science Foundation of China (Grant No: 21573075), and Shanghai Pujiang Program PJ1403500.

Notes and references

- J. S. Luterbacher, J. M. Rand, D. M. Alonso, J. Han, J. T. Youngquist, C. T. Maravelias, B. F. Pfleger and J. A. Dumesic, *Science*, 2014, **343**, 277.
- P. Ferrini and R. Rinaldi, *Angew. Chem.*, 2014, **53**, 8559.
- Y. Cheng, J. Jae, J. Shi, W. Fan and G. W. Huber, *Angew. Chem.*, 2012, **124**, 1416.
- M. Kåldström, N. Meine, C. Farès, R. Rinaldi and F. Schüth, *Green Chem.*, 2014, **16**, 2454.
- J. Zakzeski, P. C. A. Bruijninx, A. L. Jongerius and B. M. Weckhuysen, *Chem. Rev.*, 2010, **110**, 3552.
- A. Corma, S. Iborra and A. Velty, *Chem. Rev.*, 2007, **107**, 2411.
- A. Centeno, E. Laurent and B. Delmon, *J. Catal.*, 1995, **154**, 288.
- Z. Luo, Y. Wang, M. He and C. Zhao, *Green Chem.*, 2015, DOI: 10.1039/C5GC01790D.
- N. Yan, Y. Yuan, R. Dykeman, Y. Kou and P. J. Dyson, *Angew. Chem.*, 2010, **49**, 5549.
- J. He, C. Zhao and J. A. Lercher, *J. Am. Chem. Soc.*, 2012, **134**, 20768.
- A. G. Sergeev and J. F. Hartwig, *Science*, 2011, **332**, 439.
- J. M. Nichols, L. M. Bishop, R. G. Bergman and J. A. Ellman, *J. Am. Chem. Soc.*, 2010, **132**, 12554.
- S. Son and F. D. Toste, *Angew. Chem.*, 2010, **49**, 3791.
- A. G. Sergeev, J. D. Webb and J. F. Hartwig, *J. Am. Chem. Soc.*, 2012, **134**, 20226.
- E. Laurent and B. Delmon, *J. Catal.*, 1994, **146**, 281.
- A. Rahimi, A. Ulbrich, J. J. Coon and S. S. Stahl, *Nature*, 2014, **515**, 249.
- R. Ma, W. Hao, X. Ma, Y. Tian and Y. Li, *Angew. Chem.*, 2014, **53**, 7310.
- C. Crestini, M. C. Caponi, D. S. Argyropoulos and R. Saladino, *Bioorg. Med. Chem.*, 2006, **14**, 5292.
- J. M. Pepper and H. Hibbert, *J. Am. Chem. Soc.*, 1948, **70**, 67.
- D. Meier, R. Ante and O. Faix, *Bioresour. Technol.*, 1992, **40**, 171.
- Q. Song, F. Wang and J. Xu, *Chem. Commun.*, 2012, **48**, 7019.
- X. Wang and R. Rinaldi, *Angew. Chem.*, 2013, **52**, 11499.
- P. Ferrini and R. Rinaldi, *Angew. Chem.*, 2014, **53**, 8634.
- J. P. Mikkola, H. Vainio, T. Salmi, R. Sjöholm, T. Ollonqvist and J. Väyrynen, *Appl. Catal. A.*, 2000, **196**, 143.

Table of Content:

